Available online at www.sciencedirect.com
SCIENCE DIRECT®
Chemical Physics Letters 405 (2005) 53–57
CHEMICAL PHYSICS LETTERS
www.elsevier.com/locate/cplett

Low ↔ high density transformations in ice

Koichiro Umemoto *, Renata M. Wentzcovitch

Department of Chemical Engineering and Material Science, Minnesota Supercomputing Institute for Digital Technology and Advanced Computation, University of Minnesota, 421 Washington Avenue SE, Minneapolis, MN 55455, USA

Received 2 October 2004; in final form 24 January 2005

Abstract

We have used first-principles variable-cell-shape dynamics to investigate the compressive behavior of ice XI and ice VIII. We have observed direct reconstructions between these prototypical low and high density phases, in both directions. These transformations are not observed in practice, instead both forms amorphize under (de)compression. From this perspective, the amorphous can be viewed as an intermediate step in the low ↔ high density transformations. The reconstruction paths we observe bypass the intermediate amorphous phases and preserve the style of dipole ordering of the parent structure leading to metastable phases and large hystereses.

1. Introduction

Ice has an intricate phase diagram. Up to now, thirteen crystalline phases have been identified experimentally [1]. Except ice X, all others are hydrogen-bonded molecular phases. The crystalline forms Ic, IV, IX, XII, and the amorphous forms are strictly metastable. The others, particularly the low temperature forms, can remain metastable throughout large regions of the phase diagram. Broadly speaking the crystalline phases of ice can be described as follows: the low pressure forms ($P < \sim 10$ kbar) consist of a unique hydrogen bond network (1HBN). The high pressure forms ($\sim 10 < P < \sim 800$ kbar) are made up of two interpenetrating networks (2HBN). They are often referred to as self-clathrates. The highest pressure form known to date, ice X, is no longer molecular, but ionic. The molecular integrity is compromised beyond ~800 kbar. With increasing temperature, before melting, hydrogen disorder develops in the fully ordered low temperature molecular phases. Phase boundaries between low temperature phases are still largely unknown essentially because of their large metastability fields (large hysteresis).

In this Letter, we investigate by means of first principles computations the pressure induced behavior of ice XI and VIII, generically referred to as low and high density phases, respectively. Ice XI is the low temperature, low pressure, ferroelectric, and hydrogen-ordered form of common ice Ih – a typical 1HBN. Similarly, ice VIII is the low temperature, high pressure, anti-ferroelectric, and hydrogen-ordered form of ice VII – a typical 2HBN. We show that these prototypical structures transform continuously into each other upon compression or decompression while retaining their original style of electric dipole ordering. The phases found here, ice VIII-like and ice XI-like, have not been observed experimentally yet and it is unlikely they will under simple (de)compression. Instead, both ice XI [2–4] and ice VIII [5–7] are expected to amorphize inside each other's stability field. Therefore, the present study is relevant to understanding *amorphization* itself. It provides a perspective for interpreting the high pressure amorphous as intermediate phases produced in a stepwise transformation process between 1HBN and 2HBN *hydrogen-ordered* structures.

* Corresponding author. Fax: +612 626 7246.
E-mail address: umemoto@cems.umn.edu (K. Umemoto).

0009-2614/$ - see front matter © 2005 Elsevier B.V. All rights reserved.
doi:10.1016/j.cplett.2005.01.098

2. Results and discussion

Calculations were performed using Troullier-Martins pseudopotentials [8], 100 Ry as plane-wave cut-off, and the PBE functional [9] within the GGA approximation for the electronic exchange and correlation energy. Structural searches and optimizations under pressure were performed using variable cell shape molecular dynamics [10]. The unit cells of ice XI, VIII, VIII-like, and XI-like consist of four, four, two, and eight molecules, respectively. The number of **k** points in the irreducible wedge of the Brillouin zone that have been used in the calculations are six, eleven, six, and two for these phases, respectively.

Fig. 1 shows the lattice constants under compression in orthorhombic ($Cmc2_1$) ice XI. The compression mechanism changes at ~40 and ~90 kbar [11]. Up to ~40 kbar, lattice constants, (a, b, c), decrease monotonically. At ~40 kbar ice XI is already metastable with respect to ice VIII and the lattice parameter a starts increasing while the others decrease at a faster rate, particularly c. Indeed, near ~35 kbar, an incomensurate phonon instability develops, followed by the collapse of the lowest acoustic branch [3]. This multitude of unstable phonons, each one leading to a different (slightly perhaps) metastable structure, is what we refer to as amorphization [3]. Nonetheless, we compress ice XI at $T = 0$ K *statically* beyond ~35 kbar. In the absence of thermal fluctuations, ice XI remains in a situation of unstable equilibrium until a major rearrangement occurs at higher pressures. Our goal is to observe the nature of the *local* atomic arrangements that would take place if amorphization were inhibited, or equivalently, what the reconstructive path is leading to when amophization takes place. The almost obvious but nevertheless surprising answer is displayed in Fig. 2. Up to ~90 kbar, adjacent layers perpendicular to the [0 0 1] direction shift laterally with respect to each other along the [0 1 0] direction. At ~90 kbar, some hydrogen bonds break, while new hydrogen bonds reform. Then, ice XI transforms to a 2HBN structure, i.e., an ice *VIII-like* phase. Similarly to ice XI, ice VIII-like is also ferroelectric, instead of antiferroelectric like ice VIII. This is parallel to the case of disordered ice Ih; paraelectric ice Ih transforms under pressure to paraelectric ice VII preceded by an intermediate amorphous phase [14,15]. The more drastic molecular reorientation required to produce an anti-ferroelectric ice VIII structure must involve a higher energy barrier.

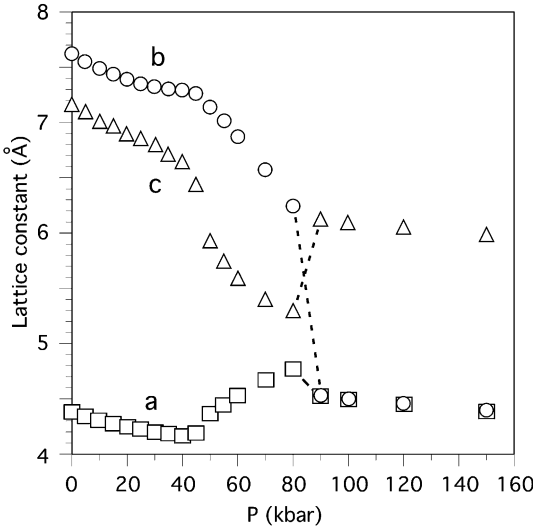

Fig. 1. Pressure dependence of lattice constants in $Cmc2_1$ ice XI.

This new high pressure structure is simple tetragonal, has two molecules per unit cell, and space group $P4_2nm$. This is a supergroup of $Cmc2_1$, the space group of ice XI [16–18]. The latter is base-centered orthorhombic containing four molecules per unit cell. A comparison between the lattice parameters of ice VIII-like and ice VIII at 100 kbar is shown in Table 1. One other difference between ice VIII-like and ice VIII is worth mentioning: the nearest neighbor arrangement. In ice VIII the interpenetrating HBN's have dipole moments oriented in opposite directions parallel to the [0 0 1] direction (see Fig. 3a). An attractive electrostatic force between these networks induces a symmetry-allowed displacement of these networks along [0 0 1] direction. This leads to a splitting of the first O–O oxygen coordination shell into three sub-shells containing two, four, and two O's [19]. Since in ice VIII-like both networks have all dipoles oriented along the same direction, this attractive interaction and the relative displacement of the networks vanish. Even if this displacement is forced, it vanishes upon structural relaxation, and the three O–O coordination sub-shells are reintegrated into a

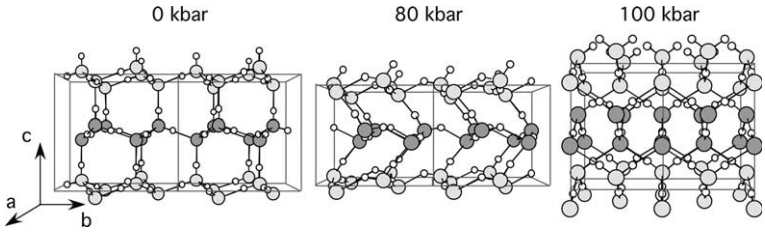

Fig. 2. Transition from ice XI to ice VIII-like phase. Small white spheres denote hydrogen atoms. Light and dark gray spheres denote oxygen atoms on different layers.

Table 1
Calculated lattice constants (Å) (upper table) and atomic coordinates (lower table)

	a	b	c
Ice VIII-like (st)	3.178	–	3.050
Ice VIII-like (bct)	4.494	–	6.101
Ice VIII (bct)	4.415	–	6.333
Ice XI-like	4.403	7.599	7.160
Ice XI	4.383	7.623	7.163
Ice VIII-like	x_H	z_H	z_O
	0.1772	0.1891	0.0000
Ice XI-like	x	y	z
H_1	0.0221	0.8079	0.2311
H_2	0.0825	0.9949	0.0491
H_3	0.4772	0.8128	0.2669
H_4	0.2939	0.9936	0.2655
O_1	0.0844	0.9961	0.1890
O_2	0.4175	0.0039	0.3139

Parameters of ice VIII-like and of ice VIII are calculated at 100 kbar and those of ice XI-like and of XI are at 0 kbar. Ice VIII-like is simple tetragonal (st) with two molecules/cell. The lattice parameters of the corresponding body-centered tetragonal (bct) lattice with four molecules/cell are also listed for comparison with ice VIII ($a_{bct} = \sqrt{2}a_{st}$, $c_{bct} = 2c_{st}$). In ice VIII-like, hydrogens and oxygens are located in 4c, (x_H, x_H, z_H) and 2a, ($0, 0, z_O$), respectively. In ice XI-like, all atoms are in 4a sites (x, y, z).

single one containing eight neighbors. As expected, the new phase is metastable with respect to ice VIII, its enthalpy being higher by 0.01 eV/molecule at 100 kbar. However, it should be stabilized with respect to ice VIII in an external electric field along [0 0 1] direction. Possibly, cooling water or paraelectric ice VII at these pressures in a field might produce this new phase. Quick dynamic compression to higher pressures, conceivably, might also produce this phase bypassing the intermediate and the amorphous phases, as well as preventing the dipoles reorientation.

Next, we consider the decompression of ice VIII. Something similar, but in the opposite direction, can now be anticipated to happen with this structure. In our previous study of ice VIII under decompression, we have correlated the unusual behavior of some phonon frequencies with specific structural features [7]: the rapid nonlinear increase of the hydrogen-bond length and decrease of the intramolecular bond length, correlates with a rapid nonlinear increase of intramolecular O–H strectching frequencies and decrease of intermolecular translational modes [20]. Lattice constants as well as hydrogen-bond lengths increase nonlinearly and we have not detected any sign of the change of compression mechanism of ice VIII as we did in ice XI. Also, the gradual softening of the two transverse acoustic branches along the entire Λ line [7] points towards amorphization [21]. At 0 kbar the frequencies of these TA phonons are not zero but 11 meV, i.e., within the energy scale in which amorphization occurs, 130 K (10.8 meV). At −12 kbar these phonons have gone completely soft, this being the sign of eminent amorphization at 0 kbar [5,6]. Here, we have annealed the structure of unstable ice VIII in the doubled unit cell, capable of the zone-edge soft mode, at $\sim$100 ± 100 K at −12 kbar for 0.4 ps and quenched rapidly. Annealing the *stretched* crystal facilitates bond breaking. *Recompression* back to 0 kbar facilitates bond reconstruction. In the first stage, half of the hydrogen bonds broke and the other half got firmer, leading to an aggregation of molecular chains extending along the [0 0 1] direction (Fig. 3). Because the structure was stretched, the broken hydrogen bonds could not reform. In the second stage, the molecular chains reconnected by new hydrogen bonds producing a hexagonal-diamond lattice, like ice XI's, but with an anti-ferroelectric type of dipole ordering, not like ferroelectric ice XI, but with the same type of ordering of the original ice VIII's structure. We call this new phase ice *XI-like*. The symmetry of ice XI-like is $P2_12_12_1$. This is the 'M' hydrogen-ordering type of ice Ih in Ref. [22]. This symmetry is different from that of another anti-ferroelectric phase considered previously by others ($Pna2_1$) [23–26]. Although ice XI-like is

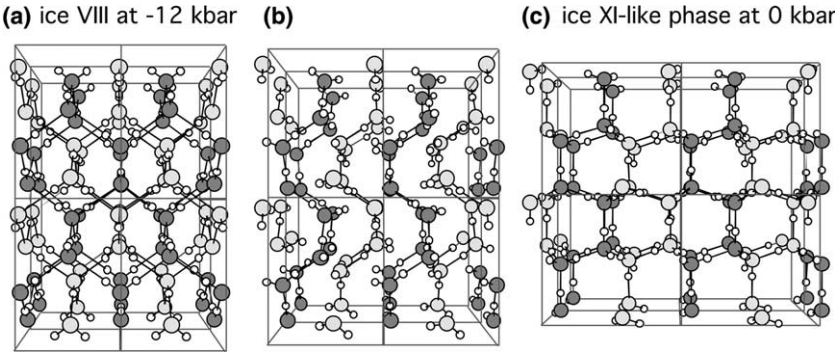

Fig. 3. Transition from ice VIII to ice XI-like. Light and dark gray spheres in (a) denote oxygen atoms on different diamond sublattices. (b) Annealed ice VIII at −12 kbar. The density is similar to ice XI's at zero pressure (see text). (c) Reconstructed hydrogen bonds forming ice XI-like.

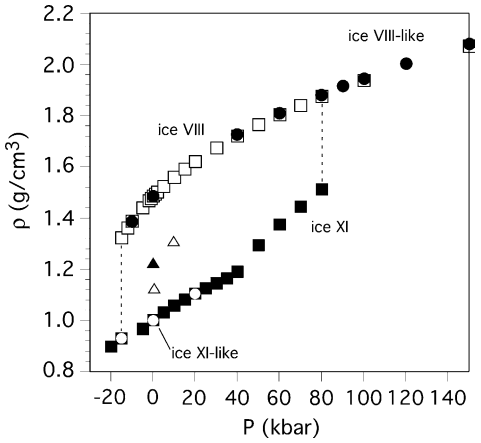

Fig. 4. Calculated densities of ice XI (■), ice VIII-like (●), ice VIII (□), and ice XI-like (○). △ and ▲ denote the experimental densities of high density (HDA) [4] and very high density amorphous (VHDA), respectively [27].

metastable with respect to ice XI, their enthalpy difference is quite small: 0.003 eV/molecule at zero pressure.

Fig. 4 shows the pressure-dependence of the densities at 0 K of the four phases under consideration. 1HBN and 2HBN phases are well separated from each other. The nearly vertical dashed lines are at the points, where structural reconstructions were observed. The final diagram has the typical form of a hysteresis loop. Experimental amorphous densities are located inside the loop. They are produced as intermediate steps in the transformation process between low ↔ high density phases. In this 0 K static (de)compression study they were suppressed though. Superposition of several unstable acoustic modes in the initial configuration of much larger sucercells followed by annealing might give a glimpse of the amorphous' atomic structure.

Although this study was carried out with relatively small numbers of atoms, the systems considered were sufficiently large to encompass both structural varieties, i.e., ferro- and antiferroelectric structures in both reconstructions. The outcome indicates instead that these transformation paths preserve the initial style of dipole ordering, even though they lead to metastable phases. Here, we are able to observe this because amorphization is inhibited by (de)compression at 0 K (without fluctuations) and relatively small supercells. We conclude that the paths for transformations involving wide reorientations of dipoles must involve larger energy barriers making these transformations more difficult to observe even if they lead to truly stable phases. Here, we are detecting what, in practice, manifests as a kinetic effect, i.e., hysteresis. Zero point motion, thermal fluctuations, or the occurrence of the intermediate amorphous might affect the *observed* transition pressures and the width of the hysteresis loop but might not affect this conclusion.

It is interesting to note that direct transitions between hydrogen-ordered phases with the same or different dipole ordering are usually suppressed, the only exception being ice IX → II under heating [28], with ice IX being metastable and not completely ordered. At the lowest temperatures, where the ordered phases exist, there are large hystereses and phase boundaries are still largely unknown (e.g., XI ↔ II ↔ VIII) [1]. Instead, transitions involving hydrogen-disordered and/or amorphous phases are the ones frequently observed, even if involving metastable phases (e.g., Ih → amorphous, VIII → amorphous → Ic → Ih under heating, etc.) [1]. Our study suggests that even paths involving intermediate amorphous phases, i.e., ordered crystal → amorphous → ordered crystal, transformations might end up in metastable phases if drastic dipole reordering is required to reach the final stable phase.

3. Conclusions

In summary, by performing static 0 K compression of ice XI and decompression of ice VIII followed by gentle annealing we have observed direct reconstructions between typical low and high density phases. These transformations are not observed in practice, instead both forms of ice amorphize under pressure or decompression inside each other's stability fields. From this perspective, the amorphous can be viewed as an intermediate step in the low ↔ high density transformations. The reconstruction paths we observe bypass the intermediate amorphous phases and preserve the style of dipole ordering of the parent phases leading to metastable phases. The preservation of the style of dipole ordering indicates that transition paths leading to dipole reordering must involve higher energy barriers and larger hystereses than those preserving the original dipole arrangement. This effect appears to be very strong to the point that the style of dipole ordering can be transmitted through the intermediate amorphous structure. For instance, paraelectric ice Ih transforms not to ferroelectric ice VIII but to paraelectric ice VII in the stability field of ice VIII, via the intermediate amorphous phase [14,15].

Acknowledgments

We thank Stefano Baroni for discussions on this topic. Calculations in this work have been done using the PWscf package [29]. This research was supported by NSF Grants No. EAR-0135533 (COMPRES), No. EAR-0230319 and No. ITR-0428774 (VLab).

References

[1] V.F. Petrenko, R.W. Whitworth, Physics of Ice Oxford, 1998.
[2] It has been predicted theoretically that ice XI should amorphize under compression [3]. This is a plausible and analogous

phenomenon to that observed in ice Ih [4]. For the sake of argument we mention this prediction as a fact here.
[3] K. Umemoto, R.M. Wentzcovitch, S. Baroni, S. de Gironcoli, Phys. Rev. Lett. 92 (2004) 105502.
[4] O. Mishima, L.D. Calvert, E. Whalley, Nature 310 (1984) 393.
[5] D.D. Klug, Y.P. Handa, T.S. Tse, E. Whalley, J. Chem. Phys. 90 (1989) 2390.
[6] A.M. Balagurov, O.I. Barkalov, A.I. Kolesnikov, G.M. Mironova, E.G. Ponyatovskii, V.V. Sinitsyn, V.K. Fedotov, JETP Lett. 53 (1991) 30.
[7] K. Umemoto, R.M. Wentzcovitch, Phys. Rev. B 69 (2004) R180103.
[8] N. Troullier, J.L. Martins, Phys. Rev. B 43 (1991) 1993.
[9] J.P. Perdew, K. Burke, M. Ernzerhof, Phys. Rev. Lett. 77 (1996) 3865.
[10] R.M. Wentzcovitch, J.L. Martins, G.D. Price, Phys. Rev. Lett. 70 (1993) 3947.
[11] The nominal pressures cited here could deviate from true value because of the limitated accuracy of our calculations: we have ignored zero-point motion, tunneling [12,13], and finite temperature effects. Nevertheless, the phenomenology uncovered here is not expected to be invalidated by these effects.
[12] M. Benoit, D. Marx, M. Parrinello, Nature 392 (1998) 258.
[13] M. Benoit, D. Marx, M. Parrinello, Comp. Mat. Sci. 10 (1998) 88.
[14] J.S. Tse, M.L. Klein, Phys. Rev. Lett. 58 (1987) 1672.
[15] R.J. Hemley, L.C. Chen, H.K. Mao, Nature 338 (1989) 638.
[16] A.J. Leadbetter, R.C. Ward, J.W. Clark, P.A. Tucker, T. Matsuo, H. Suga, J. Chem. Phys. 82 (1985) 424.
[17] C.M.B. Line, R.W. Whitworth, J. Chem. Phys. 104 (1996) 10008.
[18] S.M. Jackson, V.M. Nield, R.W. Whitworth, M. Oguro, C.C. Wilson, J. Phys. Chem. B 101 (1997) 6142.
[19] W.F. Kuhs, J.L. Finney, C. Vettier, D.V. Bliss, J. Chem. Phys. 81 (1984) 3612.
[20] J.M. Besson, S. Klotz, G. Hamel, W.G. Marshall, R.J. Nelmes, J.S. Loveday, Phys. Rev. Lett. 78 (1997) 3141.
[21] S.L. Chaplot, S.K. Sikka, Phys. Rev. Lett. 71 (1993) 2674.
[22] R. Howe, J. de Phys. 48, Colloque C1 (1987) 599.
[23] E.R. Davidson, K. Morokuma, J. Chem. Phys. 81 (1984) 3741.
[24] B.J. Yoon, K. Morokuma, E.R. Davidson, J. Chem. Phys. 83 (1985) 1223.
[25] C. Pisani, S. Casassa, P. Ugliengo, Chem. Phys. Lett. 253 (1996) 201.
[26] S. Casassa, P. Ugliengo, C. Pisani, J. Chem. Phys. 106 (1997) 8030.
[27] T. Loerting, C. Salzmann, I. Kohl, E. Mayer, A. Hallbrucker, Phys. Chem. Chem. Phys. 3 (2001) 5355.
[28] J.D. Londono, W.F. Kuhs, J.L. Finney, J. Chem. Phys. 98 (1993) 4878.
[29] S. Baroni, A. Dal Corso, S. de Gironcoli, P. Giannozzi. Available from: <http://www.pwscf.org>.